Research Article | Vol. 14, No. 6 / 1 Jun 2023 / Biomedical Optics Express 2821
Biomedical Optics EXPRESS

Approach to the design of different types of intraocular lenses based on an improved sinusoidal profile

YUWEI XING,[1] YONGJI LIU,[1,2,*] KUNQI LI,[1] XIAOLAN LI,[1] DONGYU LIU,[1] AND YAN WANG[2,3]

[1]*Tianjin Key Laboratory of Micro-scale Optical Information Science and Technology, Institute of Modern Optics, Nankai University, 38 Tongyan Road, Haihe Education Park, Tianjin, 300350, China*
[2]*Nankai University Eye Institute, Nankai University Affiliated Eye Hospital, Nankai University, 38 Tongyan Road, Haihe Education Park, Tianjin, 300350, China*
[3]*Tianjin Key Laboratory of Ophthalmology and Visual Science, Tianjin Eye Institute, Tianjin Eye Hospital, 4 Gansu Rd, Tianjin 300020, China*
[*]*yjliu@nankai.edu.cn*

Abstract: An approach is presented to design different types of Intraocular lenses (IOLs) with a uniform optimization algorithm. An improved sinusoidal phase function is proposed to realize adjustable energy allocations in different diffractive orders according to the design aims. By setting specific optimization goals, different types of IOLs can be designed using the same optimization algorithm. With this method, bifocal, trifocal, extended-depth-of-focus (EDoF), and mono-EDoF IOLs are successfully designed and their optical performance under monochromatic and polychromatic light is evaluated and compared with their commercial counterparts. The result shows that most of the designed IOLs, even though they don't have any multi-zones or combination of diffractive profiles, have superior or comparable performance to their commercial counterparts in terms of optical performance under monochromatic light. The result demonstrates the validity and reliability of the approach proposed in this paper. With this method, the development time of different types of IOLs could be reduced considerably.

1. Introduction

Surgical implantation of an Intraocular lens (IOL) is an effective way to restore the vision of cataract patients by replacing the natural crystalline lens of the human eye with IOL. The ultimate goal of IOL design is to provide a functional vision for targets at different object distances, similar to what the crystalline lens of the human eye does for young eyes [1]. Tremendous efforts have been made to achieve this goal. The IOL design has evolved from monofocal IOLs to multifocal IOLs such as bifocal and trifocal IOLs, which provide the functional vision for objects at more than one distance. To provide functional vision over a certain continuous object range, Extended-Depth-of-Focus (EDoF) IOLs were developed by increasing the depth of focus [2]. Recently, so-called Mono-EDoF [3], also known as enhanced monofocal IOLs, another group IOLs in the EDoF classification, were launched to the market, which were claimed to provide distance vision similar to a standard aspherical monofocal IOL, meanwhile, improve intermediate vision [4]. A refractive or diffractive surface is usually used to provide multifocal or extended depth of the IOLs [5]. No matter it is refractive or diffractive, the key for an IOL to achieve multifocal or EDoF function is to design the phase of the IOL, i.e. the profile of the IOL.

Refractive IOLs usually utilize segmented zones with different powers or optimized surface profiles to manipulate the specific aberrations that are usually the fourth and sixth-order spherical aberrations to finally provide multiple foci or extended depth of focus. Fernandez *et al.* [6] implemented a multi-configuration approach to optimize the aspheric coefficients of the IOL

#491762 https://doi.org/10.1364/BOE.491762
Journal © 2023 Received 27 Mar 2023; revised 12 May 2023; accepted 14 May 2023; published 22 May 2023

Biomedical Optics EXPRESS

surfaces to obtain a multifocal IOL with through-focus performance. Dai [7] employed an iterative function minimization algorithm to optimize the surface profiles, thus providing optical compensation for presbyopia. The major drawback of refractive IOLs lies in the sensitivity of their optical performance to pupil diameter changes. To overcome this drawback, diffractive IOLs have gained extensive attention. Diffractive optical element (DOE) for beam shaping techniques such as axicon [8], peacock eye [9], and light sword element [10,11]were applied to the IOL design, but such DOEs only reached limited application in human eyes. Other optimized phase plates like multiple zone multifocal phase [12], and binary-phase mask [13] also demonstrated the possibilities in the ophthalmic applications. However, the most widely used diffractive structure in commercial IOLs is the kinoform surface [14–17]. Proper optimizations are normally required to obtain multifocal or EDoF optical properties. Designing a specific type of IOL usually demands a specific optimization method such as the ones we mentioned above. To our knowledge, there is no report on designing different types of IOL using a uniform optimization algorithm along with the same phase function. Such an approach has the benefit of significantly reducing the development time of different types of IOLs.

Another essential feature of IOL is the imaging quality that determines how well the vision would be achieved after IOL implantation. The multiple foci or EDoF is achieved at the expense of a reduction in retinal image quality, which can be compensated, to some extent, by brain processing [18]. One essential way to improve the image quality of the IOLs is to increase the diffraction efficiency [15]. At present, the total diffraction efficiency of commercial trifocal IOLs with kinoform profiles is about 86%-88% [16,17]. A sinusoidal phase DOE called optimum triplicator [19], in which the input energy is equally distributed in three foci, offered a diffraction efficiency as high as 92.56%. The possibility of using such sinusoidal profiles and other sin-like profiles to design the multifocal IOLs was investigated [20–22]. Recently, commercial trifocal IOLs [23,24] with sinusoidal profiles have been launched in the market. It is claimed that IOLs with a sinusoidal profile had low halos and outstanding optical performance in all vision distances [25,26]. The sinusoidal diffractive IOLs are thus promising for providing high diffraction efficiency. However, the sinusoidal IOLs based on the optimum triplicator can only be used to design trifocal IOL, because it lacks the flexibility to allocate energy among different foci. If this limit can be overcome, it is possible to design different types of IOLs including bifocal, trifocal, EDoF, and mono-EDoF IOLs.

In this paper, we explore this possibility by making modifications to the sinusoidal phase function of the optimum triplicator. An approach is developed to design different types of commercially available IOLs implementing a uniform optimization algorithm. The optical performance of the designed IOLs is compared with their commercial counterparts.

2. Methods

2.1. Improved sinusoidal phase function

The optical features of diffractive IOLs such as bifocal, trifocal, EDoF, and mono-EDoF are mainly provided by the diffractive profile or phase function. The relationship between the phase function $\varphi(r)$ and the diffractive profile $h(r)$ can be described as follows:

$$h(r) = \frac{\lambda}{2\pi(n_2(\lambda) - n_1(\lambda))}\varphi(r), \tag{1}$$

where λ is the design wavelength, $n_1(\lambda)$ is the refractive index of the medium around the IOL, $n_2(\lambda)$ is the refractive index of the IOL material, and $\varphi(r)$ is the phase function. In this study, λ is set to 555 nm. To obtain an IOL with desired optical features, the phase function $\varphi(r)$ should be properly designed.

Biomedical Optics EXPRESS

The phase function of the optimum triplicator with a continuous sinusoidal profile, proposed by Gori *et al.* [19], is shown in the following equation:

$$\varphi(r) = \tan^{-1}(\alpha \cdot (\sin(\frac{2\pi r^2}{T})), \tag{2}$$

where r is the radial coordinate along the lens aperture, T is the period of the phase function in a unit of mm^2, and α is the parameter to control the sinusoidal amplitude. As indicated by Gori *et al.*, if α=2.65718, the triplicator provides equal diffraction efficiency for three diffractive orders with a total diffraction efficiency as high as 92.56%.

To investigate a commercial sinusoidal IOL, Vega *et al.* [21] added a shifting parameter S in the Eq. (2) to obtain a new phase function as shown in the Eq. (3):

$$\varphi(r) = \tan^{-1}(\alpha \cdot (\sin(\frac{2\pi(r^2 - S)}{T})). \tag{3}$$

The added parameter S can affect the central region profile of the whole diffractive profile. The parameter α in Eq. (3) is the only parameter that can be used to adjust the energy distribution among the intermediate (order 0) and distance (order -1), near (order +1), so that the energy percentage of the distance (order -1) and near (order +1) remains the same [19,20]. It is therefore unable to control the energy percentage of the three foci independently by using only a single parameter α. To solve this problem, we proposed a new phase function as shown in Eq. (4):

$$\varphi(r) = Po \cdot \tan^{-1}(\alpha \cdot (\sin(\frac{2\pi(r^2 - S)}{T}) + Co \cdot \sin(\frac{4\pi(r^2 - S)}{T}))). \tag{4}$$

Here, $S = S_0 \cdot T$, S_0 is a constant between 0 and 1, and an additional sinusoidal term with a period of $T/2$ has been added to the Eq. (3). A new parameter Po has also been added as an amplitude parameter for the entire sinusoidal diffractive profile and Co is the amplitude coefficient of the second sinusoidal term. In the following section, this new phase function is called the improved sinusoidal phase function and the corresponding profile is called the improved sinusoidal profile. In the present study, α is still set to 2.65718 to determine the initial structure. T depends on the expected diffractive add power P_d of the diffractive IOLs as shown by the following equation:

$$P_d = \frac{2\lambda}{T}, \tag{5}$$

where λ is the design wavelength. Thus, T is obtained from the predetermined diffractive add power P_d. Therefore, parameters Po and Co are the remained variables that allow us to control the performance of the new phase function $\varphi(r)$. Here, whether the new phase function can control the diffraction efficiency of each order independently is tested by investigating the diffraction efficiency of each order.

If a phase $\varphi(r)$ is a period function, which is the case for the phase function expressed by the Eq. (4) when r^2 is replaced by x, its diffraction efficiency of each order could be obtained by the Fourier transform. The diffraction efficiency η_m of order m is calculated according to the following equations [19,27]:

$$\tau_m = \frac{1}{T}\int_{-\frac{T}{2}}^{\frac{T}{2}} \exp[i\varphi(x)] \cdot \exp(-im\frac{2\pi x}{T})dx, \tag{6}$$

$$\eta_m = |\tau_m|^2, m = -1, 0, 1, \tag{7}$$

where $\varphi(x)$ is the phase function of the Eq. (4) with $x = r^2$, T is the period, τ_m is the Fourier coefficient, and η_m is the diffraction efficiency of order m.

Biomedical Optics EXPRESS

We set $T = 0.6285\ mm^2$ (corresponding to a diffractive add power of 1.75 D), and $S = 0$ to investigate the diffraction efficiency of each order and the total diffraction efficiency when *Po* changes from 0.6 to 1.6 and *Co* changes from -1 to +1. It is important to note that the parameter *S* does not affect the diffraction efficiency when it is calculated based on the Fourier transform of one period without considering aperture size. The diffraction efficiency of the improved sinusoidal phase function is calculated according to the Eq. (6) and (7), and the results are shown in Fig. 1(a)-(d).

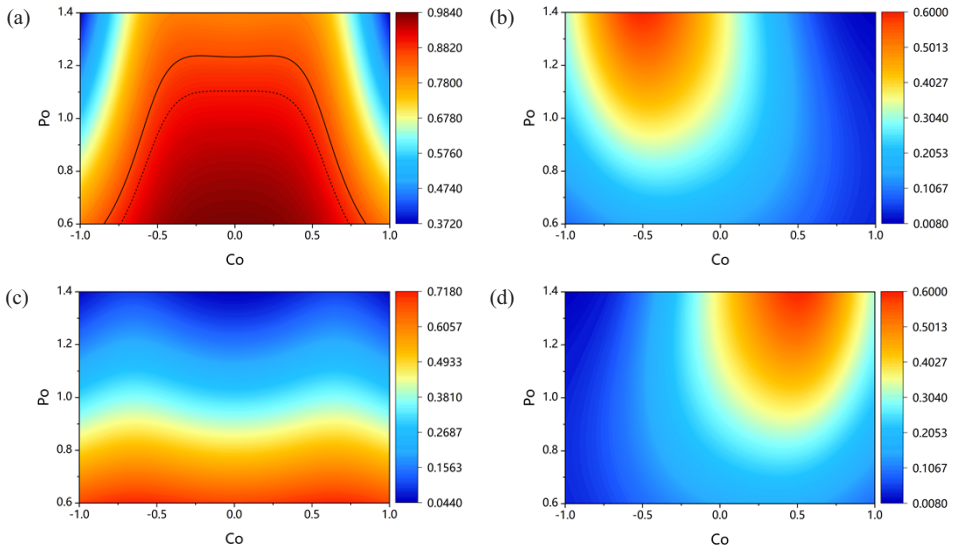

Fig. 1. The diffraction efficiency of each order and the total diffraction efficiency change with *Po*, *Co*, with $T = 0.6285\ mm^2$, $S = 0$, and α=2.65718. (a) The total diffraction efficiency. (b) The diffraction efficiency of order -1. (c) The diffraction efficiency of order 0. (d) The diffraction efficiency of order +1. The solid black curve in (a) represents the contour with a total diffraction efficiency of 0.86, and the dashed black curve represents the contour with a total diffraction efficiency of 0.90. The scale bar on the right side of each figure shows the value of total diffraction efficiency (a) and diffraction efficiency of each specific order (b)-(d).

The relationship between total diffraction efficiency and parameter *Po* and *Co* is illustrated in Fig. 1(a). Since the diffraction efficiency of the currently available commercial trifocal IOL is around 0.86 and a diffraction efficiency of 0.9 represents a high level of diffractive IOLs, the contours representing a total diffraction efficiency of 0.86 and 0.90 are illustrated in Fig. 1(a), showing that the total diffractive efficiency is jointly determined by *Po* and *Co* and that the total diffraction efficiency increases inversely with *Po*. Meanwhile, the total diffraction efficiency increases as *Co* gets closer to 0. When designing a diffractive IOL, the total diffraction efficiency should be as high as possible which means that the combination of *Po* and *Co* could not be chosen randomly. To obtain an IOL with diffraction efficiency comparable to or even better than that of the commercial IOLs, the diffraction efficiency produced by a specific combination of *Po* and *Co* should be under the contour lines as shown in Fig. 1(a). This suggests that a *Po* in the range of 0.7 to 1.3 and a *Co* in the range of -0.5 to 0.5 can give a high diffraction efficiency.

The relationship between the diffraction efficiency of each order with *Po* and *Co* are illustrated in Fig. (b) - (d), which shows that both *Po* and *Co* have an important role in the diffraction efficiency of order +1 and -1. For diffraction order 0, *Po* plays a more critical role in the diffraction efficiency than *Co*, as shown in Fig. 1(c).

Biomedical Optics EXPRESS

It is also illustrated in Fig. 1. (b) that when -1 < *Co* < 0, *Po* has a significant effect on the diffraction efficiency of order -1, showing an increase in diffraction efficiency with the increase of *Po*. When *Co* is around -0.5 and *Po* is around 1.4, the diffraction efficiency of order -1 reaches the largest value. The diffraction efficiency pattern of order +1 demonstrates the same trend except that the largest value appears for the positive *Co*. Figure 1(a-d) shows that once *Po* is set to obtain a certain diffraction efficiency for order 0, *Co* will affect the diffraction efficiency of order +1 and order -1 significantly whereas the efficiency of order 0 does not show much variation as *Co* has little effect on the efficiency of the order 0. In addition, Fig. 1(b) and (d) also demonstrates that the diffraction efficiency of the order +1 and -1 do not keep the same anymore when *Po*, *Co*, and other parameters are set as same values. This means the improved phase function allows us to control the diffraction efficiency of each order independently. By choosing a certain combination of *Po* and *Co*, a specific efficiency pattern, such as 0.4, 0.3, and 0.3 for orders of -1, 0, + 1, can be achieved.

Taken together, it is obvious that the design of a diffractive IOL with specific optical features can be transformed into searching a proper combination of *Po* and *Co*. The exact value of *Po* and *Co* will be determined through an optimization algorithm aiming for a specific IOL design, which will be in detail in section 2.3. We find that different types of diffractive IOL could be obtained by simply changing the combination of *Po*, *Co* once the specific optimization goals have been set.

2.2. Construction of the sinusoidal diffractive IOL

The material of the IOL is polymethyl methacrylate (PMMA) with a refractive index of 1.492 for 550 nm @35°C and an Abbe number of 56.8. The optical zone diameter of IOL is 6.0 mm. The design wavelength λ is set to 555 nm because the human eye is most sensitive to this wavelength.

The Liou and Brennan eye model is used to optimize the initial parameters of for the sinusoidal IOLs [28,29]. The cornea spherical aberration (SA) of this eye model for a 6 mm entrance pupil diameter is 0.26 μm. The axial length of the eye model is optimized under a pupil diameter of 3.0 mm by adjusting the vitreous chamber length to make a distant object in focus on the retina, resulting in an axial length of 23.598 mm. Then the crystalline lens of the eye model is replaced by an IOL, which is placed 0.80 mm away from the pupil [30]. The parameters of the Pseudophakic model eye are shown in Table 1. The parameters of the IOL surfaces are not shown here because they would be obtained after optimization.

Table 1. Parameters of the Pseudophakic eye model

Component	Radius (mm)	Conic	Thickness (mm)	Refractive index	Abbe number
Anterior corneal	7.77	-0.18	0.50	1.376	61.2
Posterior corneal	6.40	-0.60	3.16	1.336	55.1
Pupil	Infinity	0	0.80	1.336	55.1
Anterior IOL	-	-	0.90	1.492	56.8
Posterior IOL	-	-	-	1.336	55.1
Retina	-12.0	-	-	-	-

A sinusoidal diffractive IOL consists of a base refractive lens and a sinusoidal diffractive profile superposed on the anterior or posterior surface of the IOL. The diffractive profile provides additional focus besides the focus provided by the base refractive lens.

A refractive base lens with base power P_{base}=20+P_d D is designed firstly, where P_d is the diffractive add power. If a sinusoidal diffractive profile with a diffractive add power of P_d is superimposed on the base lens with base power P_{base}, a diffractive IOL with three powers of $P_{base}-P_d$, P_{base} and $P_{base}+P_d$ respectively, corresponding to three visual distances of far, intermediate, and near respectively, is obtained. With the base lens with a power of 20+P_d *D*,

Biomedical Optics EXPRESS

the corresponding powers of each order of the diffractive IOL are 20 D, 20+P_d D, and 20 + 2P_d D. It is worthy to note that when we design a bifocal or mono-EDoF IOL which uses only the diffractive order 0 and 1 of the sinusoidal phase, the base power P_{base} should be set to 20 D to obtain an IOL with the power of 20 D and 20+P_d D.

To reduce the fabrication difficulty, the anterior surface is an asphere with a simple conic constant and the posterior surface was a sphere. The geometry of the IOL surfaces is described by:

$$Z_1 = \frac{cr^2}{1 + \sqrt{1 - (1 + k)c^2r^2}}, \tag{8}$$

where c is the radius of curvature, and k is the conic constant, with a $k = 0$ for the posterior surface (spherical). The radii of the anterior and posterior surfaces and k of the anterior surface are optimized to obtain a biconvex base lens with power P_{base}. Meanwhile, the best MTF performance of the base monofocal lens is obtained by minimizing the RMS wavefront using the default merit function in ZEMAX.

2.3. Optimization goals of the different types of IOLs with the sinusoidal profile

The feasibility of using the improved sinusoidal profile to design different types of IOLs is demonstrated in this section.

To obtain a specific type of diffractive IOL, the first thing that needs to be settled is to set reasonable optimization goals represented by P_d and the energy percentage for three orders. The concept of how to set optimization goals is demonstrated in Fig. 2(a)-(d). The red bars on each order represent the energy percentage for three diffractive orders and the solid curves over the bars represent the through-focus curves of the energy distribution.

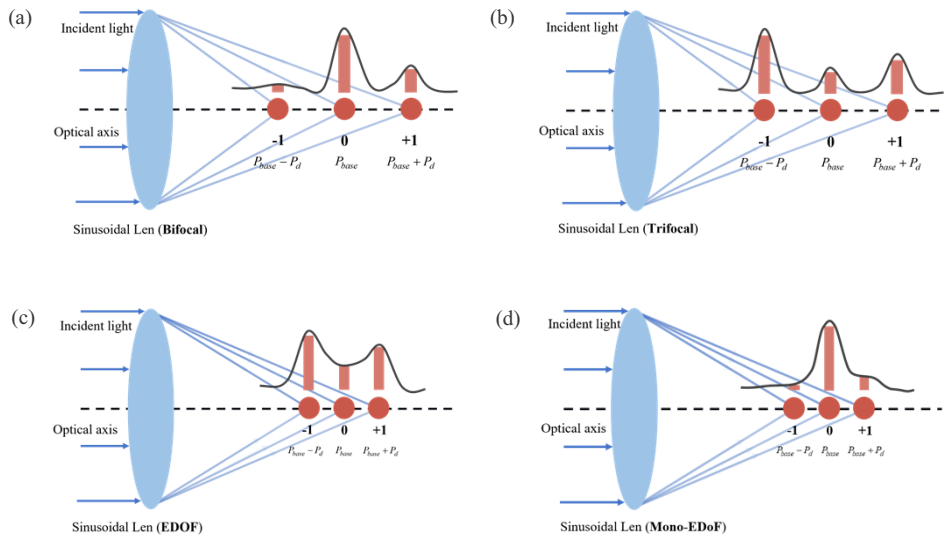

Fig. 2. Energy percentage at each focal point and through-focus curves of the energy distribution for different types of IOLs. (a) The bifocal IOL. (b) The trifocal IOL. (c) The EDoF IOL. (d) The mono-EDoF IOL. The bars above the focal points represent the energy percentage at each focal point. The solid curves over the bars represent the through-focus curves of the energy distribution.

To design a bifocal IOL, a diffractive add power P_d is usually predetermined according to the desired near working distance. Meanwhile, as shown in Fig. 2(a), the energy percentage of order -1 should be as low as possible while the energy percentage of order 0, and +1 should be as high

Biomedical Optics EXPRESS

as possible. To design a trifocal IOL, P_d is also predetermined according to the desired near working distance. The energy percentage of each order should be allocated according to actual needs. For the sinusoidal trifocal IOLs, a large percentage of energy is usually allocated to near (order +1) and far (order -1) vision, with the remaining to the intermediate (order 0) vision as shown in Fig. 2(b).

An EDoF IOL is aimed to provide a clear vision for a continuous object distance with a certain length. This is achieved by increasing the energy percentage of the intermediate vision as well as reducing the value of P_d. By doing so, the through-focus curve of the energy distribution over a certain image distance is above a specific non-zero value, demonstrating the EDoF feature as shown in Fig. 2(c). The method of designing a mono-EDoF IOL is similar to EDoF IOL, as shown in Fig. 2(d). The only difference is that a large energy percentage is allocated to the far and intermediate vision whereas the energy for near vision is reduced, intending to enhance the intermediate vision while maintaining the far vision.

From the above explanation, it is possible to design different types of IOL by changing the diffractive add power P_d and energy percentage of each order, which can be achieved by finding the proper combination of T, Po and Co. The design goals for each type of IOL are listed in Table 2.

Table 2. The energy percentage of each diffractive order and P_d for different types of IOL

IOL type	The energy percentage for each diffractive order			P_d (D)
	Order -1 (%)	Order 0 (%)	Order +1 (%)	
Bifocal	5	70	25	2.50
Trifocal	50	20	30	1.75
EDoF	45	20	35	0.85
Mono-EDoF	5	75	20	0.40

T is set according to Eq. (7) once the diffractive add power P_d is chosen. We set the initial values of other parameters as $Po = 1$, $Co = 0$, $S = 0$, and α=2.65718. Therefore, the initial phase function and the initial diffractive profile can be obtained. Such initial diffractive profile is imported into the Zemax Optical Studio (22.2 Premium, Washington Zemax LLC, USA) using User Defined Surface (UDS) [31,32] and superimposed to the posterior surface of the base lens of the pseudophakic eye model. As a result, a pseudophakic eye model with diffractive IOL had been built in Zemax.

To achieve the specific optical feature, the diffractive profile of the IOL needs to be optimized. Parameters Po and Co are set as variables to control the energy percentage of each focus and the energy distribution. Though S does not affect the diffraction efficiency in the calculation above, it affects the optical performance of the diffractive IOL which includes a refractive base lens with the aperture size. Thus, S is also set as a variable during the optimization.

In the design of diffractive IOLs, the energy percentage at each focus is mainly determined by the diffraction efficiency [33,34]. Compared with diffraction efficiency, the Modulation Transfer Function (MTF) is more comprehensive to evaluate the imaging characteristics of the designed IOL at each focus. MTF shows a behavior concerning the distribution of diffraction efficiency and can be quickly calculated by Zemax [15]. Therefore, MTF @ 50 lp/mm at the design wavelength λ=555 nm is used during the optimization for convenience. The pupil diameter is also set as 3.0 mm during the optimization. The total MTF is defined as a sum of the MTF@ 50 lp/mm of each focus, and the percentage of the MTF at each focus to the total MTF represents the energy percentage at each focus. The detailed design goals based on MTF are shown in equations (9-11):

$$MTF_{Total} = MTF_{Far} + MTF_{Intermediate} + MTF_{Near}, \tag{9}$$

$$Diff_1 = |Aim_1 - MTF_{Intermediate}/MTF_{Total}|, \tag{10}$$

Biomedical Optics EXPRESS

$$Diff_2 = |Aim_2 - MTF_{Near}/MTF_{Total}|, \tag{11}$$

where MTF_{Far}, $MTF_{Intermediate}$, MTF_{Near} corresponds to the MTF@ 50 lp/mm for far, intermediate, and near distance respectively, and MTF_{Total} is the sum of MTFs of these foci. Aim_1 and Aim_2 are the distribution goals for intermediate and near focus corresponding to the design goals in Table 2. $Diff_1$ and $Diff_2$ represent the difference between the actual energy percentage and the goals for intermediate and near focus. The ultimate goal of the optimization is to obtain a maximized MTF_{Total} with minimized $Diff_1$, $Diff_2$.

ParetoSearch algorithm is implemented to optimize the diffractive profile to determine the value of Po, Co, S. We chose this algorithm because it is a novel multi-objective derivative-free approach, called direct multi-search (DMS), which does not aggregate any of the objective functions [35]. The algorithm is run in MATLAB (MathWorks, Natick, MA, USA). MATLAB is interconnected with Zemax through an application programming interface (API) to read the MTF of the diffractive IOL in real-time.

After optimization, four types of IOLs, namely bifocal, trifocal, EDoF and mono-EDoF IOLs, are obtained. The optical performance of each type of IOL with design wavelength under different pupil diameters is evaluated in the Pseudophakic eye model shown in Table 2. In addition, the optical performance under polychromatic light is also evaluated in the same Pseudophakic eye model. The wavelength ranges from 475 nm to 645 nm with a step of 10 nm [36]. Weights are assigned to each wavelength based on the spectral luminous efficiency function for photopic vision [37].

To further demonstrate the optical performance of the IOLs obtained from this new method, the designed IOLs are compared with their commercial counterparts, whose data are available in the literature [38–42]. The measuring conditions of the commercial IOLs are summarized in Table 3. The defocus values are referred to the IOL plane. The optical performance of the designed IOLs is evaluated in the same conditions as those in which their commercial counterparts are measured. For example, when the optical performance of the designed bifocal IOL is compared with Restore +2.5 D, the designed bifocal IOL is evaluated in the ISO 2 eye model with +0.20 µm spherical aberration under a wavelength of 550 nm. Whereas, the designed Mono-EDoF IOL is evaluated in the ISO 2 eye model with +0.28 µm spherical aberration under a wavelength of 546 nm because it is the condition in which its commercial counterparts are measured.

Table 3. The measured conditions of the compared commercial IOLs

IOL types	Commercial IOL	Source wavelength	Eye model	Spherical aberration of the eye model cornea
Bifocal	RESTOR +2.5D	550nm	ISO 2 eye model	+0.20 µm
Trifocal	AT LISA tri			
	FineVision			
EDoF	Symfony	545nm		+0.28 µm
	AT LARA			
Mono-EDoF	Vivity	546nm		
	Eyhance			
	Acunex Quantum			

3. Results

3.1. Results of designed four types of IOL

According to the design goals in Table 2, four different types IOLs, namely bifocal, trifocal, EDoF and mono-EDoF IOLs were optimized. The diffractive profile parameters of each type of

Biomedical Optics EXPRESS

IOL are listed in Table 4. The designed bifocal IOL had a diffractive add power P_d of 2.50 D. The designed trifocal IOL had +3.50 D near diffractive add power and +1.75 D intermediate diffractive add power. It can be seen that using different combinations of the *Po*, *Co*, and *T*, different types of IOL could be designed.

Table 4. The parameters of the diffractive profile for the designed four types of IOL

IOL type	*Po*	*Co*	S_0	$T(mm^2)$	$P_d(D)$
Bifocal	0.600	0.450	0.800	0.444	2.50
Trifocal	1.180	-0.204	0.422	0.634	1.75
EDoF	1.250	0.100	0.380	1.306	0.85
Mono-EDoF	0.760	0.750	0.410	2.775	0.40

The diffractive profiles of the four IOLs are shown in Fig. 3. Figure 3(a) demonstrates an intensive diffractive profile which is the result of a large P_d. As shown in Fig. 3(b), the trifocal IOL with a P_d of 1.75 D had a relatively less intensive profile in comparison with the bifocal IOL. For the EDoF and mono-EDoF IOLs as shown in Fig. 3(c) and (d), the diffractive profiles become sparser mainly due to a decrease in P_d.

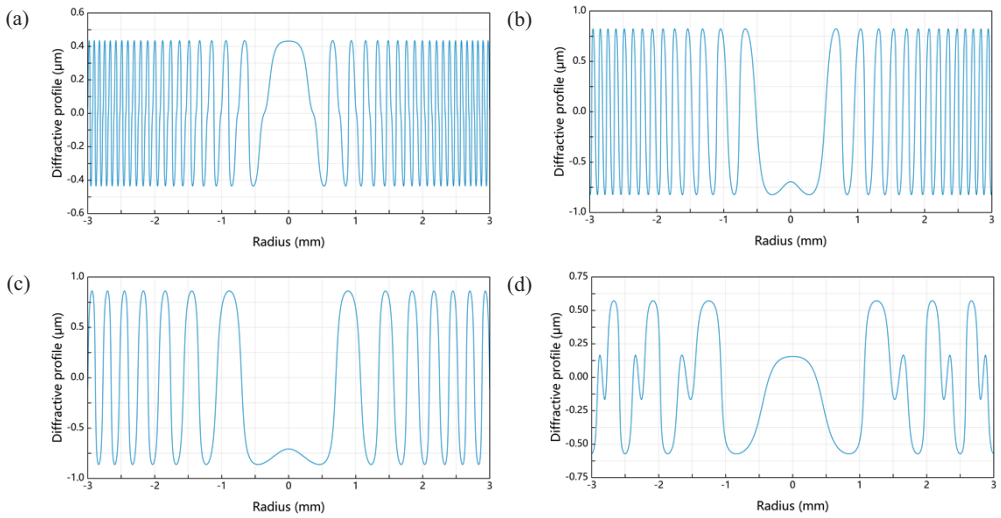

Fig. 3. Diffractive profiles (remove the base radius) of the designed IOLs. (a)The bifocal IOL. (b)The trifocal IOL. (c) The EDoF IOL. (d) The mono-EDoF IOLs.

3.2. Optical performance of the designed IOLs under monochromatic light

In this section, the optical performance of the design IOLs was demonstrated by comparing them with the corresponding commercially available IOLs. Figure 4 shows the optical performance of the designed bifocal IOL. The through-focus MTF curve at 50 lp/mm in Fig. 4(a) shows two peaks under different pupil diameters, demonstrating a bifocal characteristic. It also shows that the diffractive add power is about 2.40 D, slightly lower than the target value of 2.50 D. The optical performance of the designed bifocal IOL was compared with the AcrySof IQ ReSTOR +2.5 D (Alcon Laboratories, Fort Worth, TX, USA), which had a combination with an apodized diffractive zone and refractive zone. The results are shown in Fig. 4(b). In comparison with the ReSTOR +2.5 D (measured in the ISO 2 eye model with the spherical aberration of 0.20 μm [38]), the present bifocal design slightly improved the MTF for both far vision and near vision.

Biomedical Optics EXPRESS

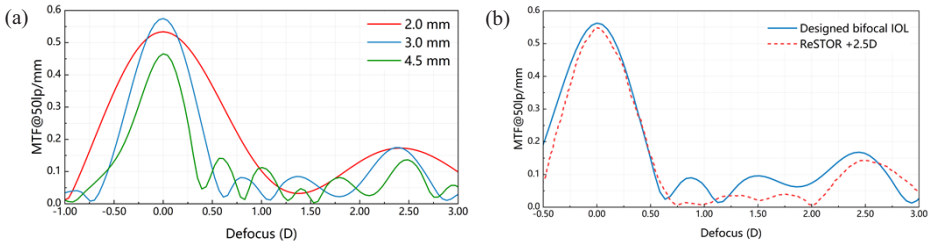

Fig. 4. Through-focus MTF curves @ 50 lp/mm of the designed bifocal IOL. (a) under pupil diameter of 2.0, 3.0, and 4.5 mm. (b) Comparison with ReSTOR +2.5 D under a pupil diameter of 3.0 mm. The data of ReSTOR +2.5D was measured in ISO 2 eye model with +0.20 μm SA.

Figure 5 shows the through-focus MTF curves of the designed trifocal IOL, demonstrating trifocal characteristics with diffractive add powers of 1.75 D and 3.50 D under the 3.0 mm pupil diameter, which meets the design goals. The performance of the designed trifocal IOL under pupil diameters of 2.0, 3.0, and 4.5 mm was investigated and results are shown in Fig. 5(a). The peak of MTF at each focus plane of the designed IOL was affected by pupil diameter. When the pupil increases, the value of MTF for the far vision remained nearly unchanged. Under a pupil diameter of 2.0 mm, the through-focus MTF demonstrated a characteristic of an EDoF IOL with a large depth of focus from 0 D to 4.0 D, corresponding to a depth of focus up to 3.0 D at the corneal plane, suggesting that the functional vision is obtained over an object distance from 33 cm to infinity.

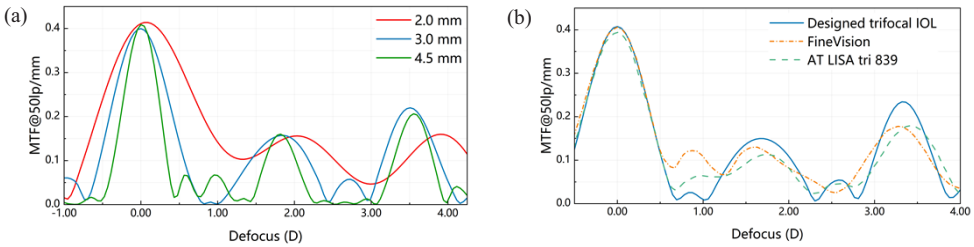

Fig. 5. Through-focus MTF curves @ 50 lp/mm of the designed trifocal IOL. (a) under pupil diameter of 2.0, 3.0, and 4.5 mm. (b) Comparison with AT LISA tri 839 and FineVision under pupil diameter of 3.0 mm. The data of AT LISA tri 839 and FineVision was measured in an ISO 2 eye model with +0.20 μm SA.

The optical performance of the designed trifocal IOL was compared with two trifocal IOLs on the market under 3.0 mm pupil diameter. One was FineVision Micro F (PhysIOL SA, Liège, Belgium), a trifocal IOL with superimposing two bifocal profiles [16], and the other one was AT Lisa Tri 839 MP (Carl Zeiss Meditec AG, Jena, Germany), which has implemented a trifocal profile in the central 4.34 mm zone and a bifocal profile outside [39]. The comparison of the designed trifocal IOL with the commercial IOLs (also measured in the ISO 2 eye model with the spherical aberration of 0.20 μm [39]) is shown in Fig. 5(b). It can be seen that the designed trifocal IOL showed a significant improvement in MTF for near vision in comparison with the AT LISA and FineVision. The MTF for the far and intermediate vision was nearly at a similar level as that of AT LISA and FineVision.

The optical performance of the designed EDoF IOL as shown in Fig. 6 demonstrates that the through-focus MTF curves under different pupil diameters. The designed EDoF IOL under 3.0 mm pupil diameter shows the expected EDoF performance with a large range of continuous vision

Biomedical Optics EXPRESS

distance. When the pupil diameter was reduced to 2.0 mm, there was an improvement in the far vision and intermediate vision whereas there was a reduction in near vision. When the pupil diameter reaches 4.5 mm, a trifocal feature appears with an increase in MTF for intermediate near vision. The through-focus MTF curves of the designed EDoF IOL under 3.0 mm pupil diameter (in vitro data measured in ISO 2 eye model with +0.28 μm SA [43]) were compared with two commercial EDoF IOLs, the TECNIS Symfony ZXR00 (Johnson & Johnson IOLs, Groningen, The Netherlands) which is based on an achromatic diffractive surface with an echelette design, and the AT LARA 829 MP (Carl Zeiss Meditec AG, Jena, Germany) which is a diffractive design with smooth microphase (SMP) [44]. The results are shown in Fig. 6(b). The designed EDoF IOL demonstrated a similar depth of focus to that of the Symfony. However, the MTFs for far and near vision were below these of Symfony. Compared to the AT LARA, the designed IOL had an increased MTF for far and near vision whereas a decreased MTF for the defocus ranged from 0.74D to 1.42D.

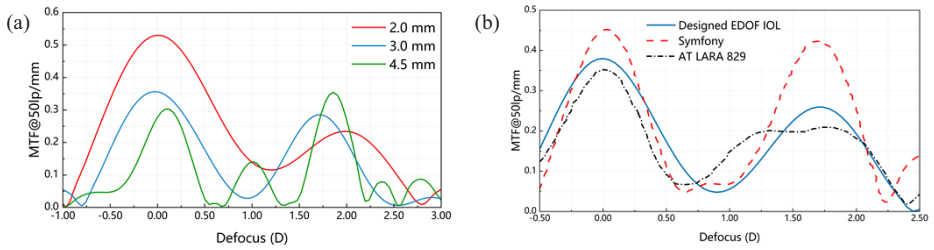

Fig. 6. Through-focus MTF curves @ 50 lp/mm of the designed EDoF IOL. (a) under pupil diameter of 2.0, 3.0, and 4.5 mm. (b) Comparison with Symfony and AT LARA under pupil diameter of 3.0 mm. The data of Symfony and AT LARA were measured in ISO 2 eye model with +0.28 μm SA.

Figure 7 shows the through-focus MTF curves of the designed mono-EDoF IOLs. The performance of the designed mono-EDoF IOL under different pupil diameters is presented in Fig. 7(a). The designed mono-EDoF IOL shows the expected mono-EDoF performance at 3.0 mm pupil diameter, enhancing intermediate vision while maintaining far vision in terms of MTF. When the pupil diameter decreases, the through-focus MTF curves tend to have a monofocal IOL performance, but with a large depth of focus. When the pupil diameter increases to 4.5 mm, it shows a trifocal characteristic but the focus of order -1 does not contribute to functional vision.

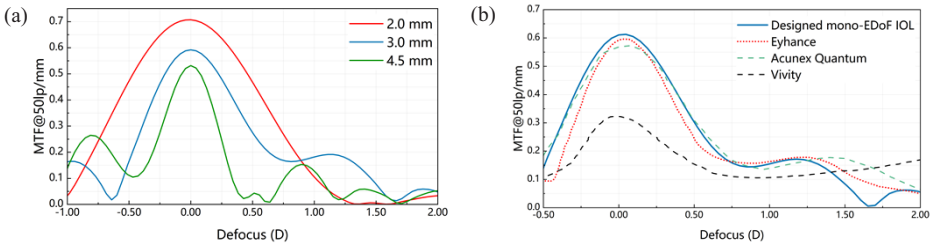

Fig. 7. Through-focus MTF curves @ 50 lp/mm of the designed mono-EDoF IOL. (a) under pupil diameter of 2.0, 3.0, and 4.5 mm. (b) Comparison with Eyhance, Acunex Quantum and Vivity under pupil diameter of 3.0 mm with monochromatic light. The data of Eyhance, Acunex Quantum and Vivity with monochromatic light was measured in ISO 2 eye model with +0.28 μm SA.

The optical performance of the designed mono-EDoF IOL was compared with an enhanced monofocal refractive IOL, the TECNIS Eyhance ICB00 (Johnson & Johnson IOLs, Groningen,

Biomedical Optics EXPRESS

The Netherlands), a mono-EDoF IOL, Acunex Quantum AN6Q (Teleon Surgical, Spankeren Netherlands) and an EDoF IOL, the AcrySof IQ Vivity DFT015 (Alcon Laboratories, Fort Worth, TX, USA), which was usually used to compare with mono-EDoF IOL [42]. The results are shown in Fig. 7(b). The MTFs of the designed mono-EDoF IOL for far vision and intermediate vision are similar to these of Eyhance and Acunex Quantum up to a defocus of 1.25D. The designed mono-EDoF IOL has a depth of focus of about 1.50 D, which is less than that of Eyhance and Acunex Quantum. Compared to Vivity, the designed mono-EDoF IOL provides better far and intermediate vision until a defocus of 1.40D (especially in 0D), but Vivity has a larger depth of focus.

3.3. Optical performance of the designed IOLs under polychromatic light

Since the Pseudophakic eyes normally work in chromatic light, the chromatic aberrations should play a role in the optical performance of the Pseudophakic eyes. To investigate the effects of longitudinal chromatic aberrations (LCA) on the optical performance of the Pseudophakic eyes implanted with the designed IOLs, the through-focus MTF curves were evaluated under polychromatic light in the Pseudophakic eye model. Because the parameters of the Eyhance IOL are available in a U.S. patent [45], the through-focus MTF under polychromatic light of the Eyhance was also evaluated in the Pseudophakic eye model. The results are shown in Fig. 8.

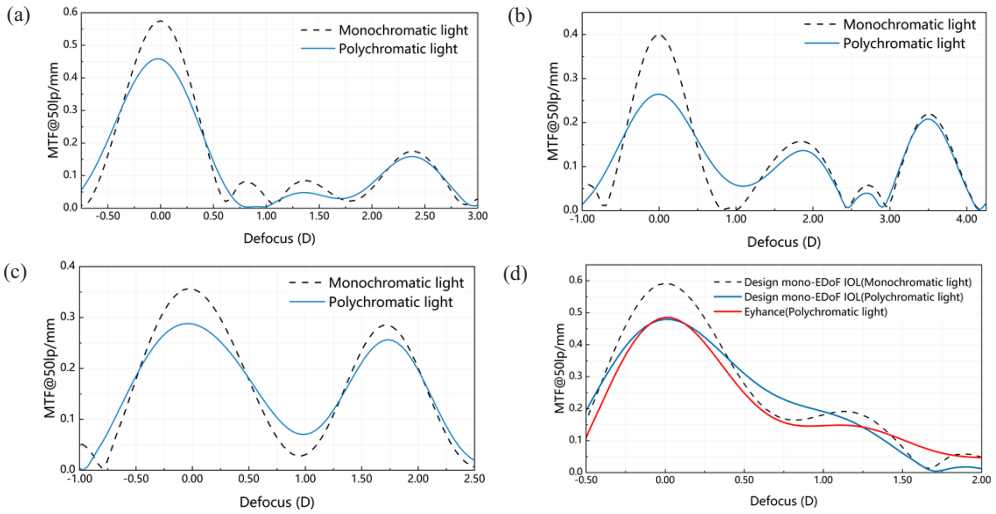

Fig. 8. Through-focus MTF curves @ 50 lp/mm of the designed IOLs with monochromatic light and polychromatic light under a pupil diameter of 3.0 mm. (a)The bifocal IOL. (b)The trifocal IOL. (c) The EDoF IOL. (d) The mono-EDoF IOL along with Eyhance with polychromatic light. All the results were obtained based on the Pseudophakic eye model.

It can be seen from Fig. 8(a-d) that the LCA caused a significant decrease in MTF for the far vision of Pseudophakic eyes implanted with each of the designed IOLs. The far vision of the Pseudophakic eye with trifocal IOL was affected by the LCA the most among all the designed IOLs, showing a decrease of 0.135 (33.81%) in the MTF for far vision. Whereas the decrease in the MTF for the far vision of the Pseudophakic eye implanted with the bifocal, EDOF and Mono-EDoF IOLs is 0.117 (20.35%), 0.068 (19.18%) and 0.112 (18.90%) respectively, demonstrating a decrease at a similar level. The LCA only slightly affected the MTF for the near vision of the Pseudophakic eye with the bifocal and trifocal IOLs. Figure 8(b) shows that the LCA caused an MTF decrease of 0.021 (13.10%) for the intermediate vision of the Pseudophakic eye with the trifocal IOL. It is worth to note that an extended depth of focus between the far

Biomedical Optics EXPRESS

vision and intermediate vision of the Pseudophakic eye with trifocal IOL was observed with polychromatic light. Figure 8(c) shows a decrease of 0.029 (10.15%) for the near vision with the EDoF IOL, which used diffractive order +1 for the near vision.

One distinct characteristic demonstrated by Fig. 8(d) is that the MTF of the designed Mono-EDoF IOL at defocus ranging from 0.42 D to 1.02 D showed an increase rather than a decrease under polychromatic light, though LCA caused a decrease in the MTF for far vision. The LCA plays a role in decreasing the MTF for the far vision, which is similar for both the designed Mono-EDoF IOL and Eyhance. The through-focus curve of the MTF of the designed mono-EDoF IOL is higher than that of the Eyhance for defocus ranging from 0.20 D to 1.25 D. The MTF of the designed mono-EDoF IOL is lower than that of the Eyhance for defocus larger than 1.25D under polychromatic.

4. Discussion

We have proposed an approach to design different types of diffractive IOLs using the same optimization algorithm. This is possible because we improved the phase function simply by adding an extra parameter in the phase function proposed by Vega *et al.* [21]. This improved phase function holds the advantage that the energy percentage at each focal point could be adjusted freely and easily by the proper combinations of the parameters in the phase function. The approach proposed in this paper makes it easier to design different types of commercially available diffractive IOLs, including bifocal, trifocal, EDoF, and mono-EDoF IOLs.

The sinusoidal profile has already been used to design IOLs, but only in multifocal IOLs (trifocal or pentafocal) to our knowledge [21,26]. Our improved sinusoidal profile makes it possible to design a variety of IOLs, thus extending the application of the sinusoidal profile in the design of IOLs.

More importantly, we found that the optical performance of designed IOLs under monochromatic light is either superior (bifocal and trifocal IOLs) or comparable to most of the commercially available counterparts studied in this paper. One thing worth pointing out is that the optical performance of the designed IOLs is achieved by a uniform sinusoidal profile without any multi-zones or combination of diffractive profiles, which is usually done for commercial counterparts, such as FineVision and Synergy [1]. By multi-zones or combination of diffractive profiles, more parameters are introduced so that more design freedoms for optimization were available to achieve certain optical performance of the IOL. If the multi-zones or combination of diffractive profiles is used on the sinusoidal profile proposed in the present study, it may be possible to further improve the optical performance of the designed IOLs. One example had been given in the following part.

The LCA of a Pseudophakic eye is the sum of the LCA introduced by the cornea, the base lens of the IOL and the diffractive profile. The LCA introduced by the diffractive order +1, has the opposite sign of the LCA introduced by the cornea and base lens. These LCAs with opposite signs could cancel out or partly cancel out each other, resulting in a small LCA for the Pseudophakic eye. This explains why the MTFs for the near vision of the Pseudophakic eye with bifocal, trifocal or EDOF IOL, which used diffractive order +1 for near vision, are only slightly affected by the LCA as shown in Fig. 8(a)-(c). Figure 8(a) and Fig. 8(d) demonstrated a drop in MTF for the far vision of the Pseudophakic eye with bifocal or Mono-EDoF IOL, which both used the diffractive order 0 for the far vision. This drop in the MTF for the far vision is due to the LCA introduced by the cornea and the base lens of the IOL, whose LCAs have the same sign. Both the trifocal and the EDoF IOL use the diffractive order -1 for far vision, but the LCA seems to have different effects on the MTF of the Pseudophakic eye with trifocal and EDoF IOLs. The diffractive order -1 will introduce an additional LCA besides the LCA introduced by the cornea and the base lens of the IOL as they have the same sign, therefore resulting in a further drop in the MTF. This was observed in the Pseudophakic eye with the trifocal IOL, which has the highest

Biomedical Optics EXPRESS

drop of 0.135 (33.81%) in the MTF for far vision among all the designed IOLs. However, the LCA only introduced a 0.068 (19.18%) drop in the MTF of the Pseudophakic eye with the EDoF IOL, which is similar to the drop for the Pseudophakic eye with bifocal or Mono-EDoF IOLs. These results suggest that for the Pseudophakic eye with the EDoF IOL, there may be a balance between LCA and monochromatic aberrations, thus reducing the effect of LCA on MTF for the far vision, though diffractive order -1 provides an extra LCA [46,47].

We were unable to obtain the optical performance of the commercial trifocal IOLs under polychromatic light in the Pseudophakic eye, therefore we could not directly compare the optical performance of the designed trifocal IOL and AT LISA or FineVision under polychromatic light. Results shown in Fig. 8(b) demonstrated that the LCA introduced by the diffractive order -1 caused a further decrease in the MTF for Pseudophakia eye with the designed trifocal IOL. This result implies that the MTF for the far vision under polychromatic light of the designed trifocal IOL seems inferior to that of the commercial trifocal IOLs like AT LISA and Fine Vision, which use the diffractive order 0 far vision.

One possible way to solve this problem is to introduce multi-zones to the sinusoidal profile. We use a zonal design that combines two bifocal (using diffractive orders 0 and +1) improved sinusoidal diffractive profiles which have different diffractive add power. As shown in Fig. 9(a), the inner zone provides far and intermediate vision (0D and +1.75D) and the outer zone provides far and near vision (0D and +3.50D). With this design, the use of diffractive order -1 for the far vision and therefore the MTF degradation due to LCA introduced by the -1 diffractive order are avoided. Figure 9(b) shows the comparison of the performance of the designed zonal trifocal IOL under monochromatic and polychromatic light. The LCA only lend to a drop of 0.057 (14.56%) in the MTF for the far vision. Compared to the previous trifocal design with a drop of 0.135 (33.80%) in the MTF, the impact of LCA is significantly reduced. This example also demonstrates that using a more complex improved sinusoidal profile could further improve the optical performance of the designed IOLs. However, the introduction of the design with multi-zones may result in abrupt changes in the height of a profile at the intersection of different zones as shown in Fig. 9(a).

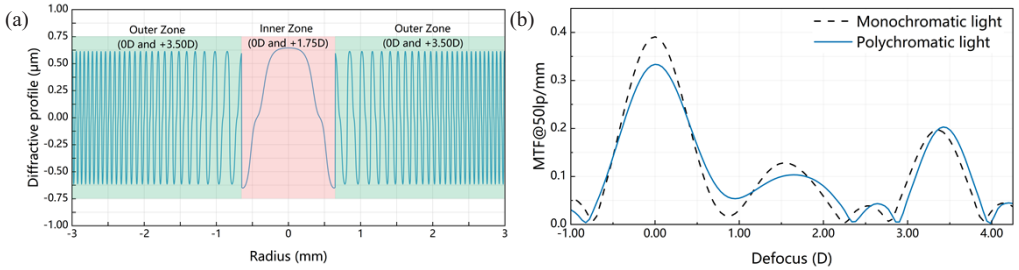

Fig. 9. The designed zonal trifocal IOL. (a) Diffractive profile (remove the base radius). (b) Through-focus MTF curves @ 50 lp/mm with monochromatic light and polychromatic light under a pupil diameter of 3.0 mm. The evaluation was conducted in the Pseudophakic eye model.

Here is one important thing worth pointing out is that visual performance involves neural processing [48] rather than solely determined by optical performance. The reports on the effects of LCA on visual performance remain controversial. Some studies reported an improvement in visual acuity after correcting LCA [46,49], whereas other studies demonstrated that visual performance was not significantly improved with the correction of LCA [48]. It seems that the retinal image degradation induced by LCA does not lead to an equal proportional degradation in visual acuity [50], probably due to the neural adaptation. Figure 8 shows that the LCA mostly affects the MTF for the far vision of the Pseudophakic eye implanted with the trifocal IOL,

Biomedical Optics EXPRESS

leading to a drop of 0.135 (33.81%). It seems that LCA may significantly affect the far vision of the eyes implanted with the designed trifocal IOL. However, the clinical study on the comparison between Acriva Trinova MIOL(VSY, Biotechnology, The Netherlands), which uses diffractive order -1 for far vision, and Fine Vision (PhysIOL, Liège, Belgium) that uses 0 order for far vision showed similar corrected visual performance for far distances [25]. This result seems to suggest that the extra LCA introduced by the diffractive order -1 does not lead to significant decrease in visual performance and contrast sensitivity, although it induces a decrease in MTF.

The IOLs, which enhance the intermediate vision while providing far vision similar to monofocal IOLs, are usually called enhanced monofocal IOLs. The Eyhance, which is a refractive design, is a typical example of this category. It is not clear whether the name "enhanced monofocal" specifically refers to the refractive design. However, it is known that the enhanced monofocal IOL is another group of IOLs within the EDoF classification [3]. As a result, the so-called "enhanced monofocal" is also known as "mono-EDoF". To avoid confusion with the enhanced monofocal IOLs that are based on refractive design, the designed IOL in this paper, which aims to improve the intermediate vision along with providing far vision similar to monofocal IOL, is called mono-EDoF IOL. Our study shows that the improved sinusoidal diffractive surface, in addition to the refractive surface, can also be used to improve the intermediate vision while keeping far vision similar to monofocal IOLs in terms of MTF performance. One possible disadvantage of the diffractive design lies in that the stray rays caused by the diffractive structure may lead to dysphotopic phenomena [51], which could be avoided by the IOL with refractive design.

The distinct difference between the sinusoidal diffractive profile to other commonly used diffractive profiles such as kinoform or binary is that the sinusoidal diffractive profile could give a smooth change in the height of the diffractive surface, whereas there are serials of abrupt changes in the height of the kinoform or binary profiles [14,52,53]. Even if the sinusoidal design has multi-zones, like what was shown in Fig. 9, abrupt changes in profile height may only appear at the intersections of different zones. In general, the number of abrupt changes remains less than the conventional diffractive profiles. This characteristic of a smooth profile may reduce the deviations of the manufactured IOLs from the designed IOLs. The diffractive profile of the IOLs is usually fabricated by single-point diamond-turning technology. Ideally, the manufactured IOL is identical to the designed one. However, deviations from the design are unavoidable. These deviations are usually introduced during the diamond-cutting process and polishing process. In the diamond-cutting process, the diamond tool has a limited size, it may be easier to produce a continuous and smooth profile of the sinusoidal diffractive IOLs than to produce a profile with abrupt changes such as the traditional kinoform, and binary profiles [54]. More importantly, the polishing process will introduce less deviations to the continuous profile than to the profile with abrupt changes. In terms of this, the sinusoidal diffractive profile seems to outperform the diffractive profile with abrupt changes.

In addition, a smooth profile of sinusoidal IOL may have the advantage to reduce the incidence of posterior capsule opacification (PCO), a long-term complication of pseudophakic presbyopia correction, which decreases the contrast sensitivity defocus curve after implantation of IOLs [55]. It was previously reported that the incidence of PCO correlates with an increase in the micro-roughness of the IOL surface [56]. Therefore, the smooth and continuous sinusoidal profile may be able to help reduce the incidence of PCO.

The damped least square (DLS) algorithm provided by Zemax is usually a powerful algorithm for optimization once a proper merit function is set. However, we observed that this DLS algorithm failed to get a convergent result for the optimization goals, and we thus used the global algorithm ParetoSearch in this study. Due to the range of optimization parameters was not large, the global algorithm was able to traverse all cases fast to find the right combination of parameters, avoiding any local optimum results. The optimization results can be performed to show 60 Pareto

Biomedical Optics EXPRESS

solutions from the ParetoSearch algorithm, allowing us to find the optimum result easily. Besides, the global algorithm ParetoSearch can be easily used by interconnecting it with Zemax once it has been programmed.

There are also some limitations in this study. We mainly demonstrated the key characteristics of the IOLs: the through-focus MTF with monochromatic light and polychromatic light. Though such analysis is reasonable because commercial IOLs are normally evaluated under monochromatic light according to ISO11972-2: 2014, more factors need to be further considered for real applications [57]. The individual variability in corneal spherical aberration will affect the optical performance of the pseudophakic eye. When an IOL is implanted inside the eye, there is usually decentration and tilt which will affect the visual quality after surgery [58]. In addition, the stray light introduced by the sinusoidal diffractive structure of the IOL may affect the optical performance of the Pseudophakic eyes. These factors need further investigation to ensure a satisfied vision after IOL implantation. As previously mentioned, implementing diffractive order -1 for far vision would introduce an extra LCA, which may influence the visual function after surgery. It deserves further efforts to investigate this problem. Another limitation of this study is that the optical performance of the commercial IOLs was obtained from the literature. Though best efforts have been made to ensure the optical performance were compared under the same situation as the commercial IOLs, manufacturing the designed IOLs and then comparing the optical performance with their commercial counterparts on the optical bench is the most convincing way to evaluate their actual performance. Because our work mainly focuses on the feasibility of the approach to design different types of IOLs, the exploration of the above limitations would be considered in our further work.

5. Conclusion

In this paper, an improved sinusoidal diffractive phase function has been proposed for the first time, which provides the flexibility in the adjustment of the energy percentage on each diffractive order. With this improved phase function, we have proposed an approach to design different types of IOLs. Four types of IOLs, i.e. bifocal, trifocal, EDoF and mono-EDoF IOLs have been obtained. The optical performance of most designed IOLs is either superior or comparable to their commercial counterparts under monochromatic light, proving the effectiveness and reliability of the approach.

Funding. National Key Research and Development Program of China (No. 2022YFC2404502); National Natural Science Foundation of China (No. 82271118); Nankai University Eye Institute (NKYKD202201); Tianjin Eye Hospital Optometric Center Science and Technology Fund (SGZX-2022-KY-00022).

Acknowledgments. All authors acknowledge the reviewers for the constructive suggestions to improve the work in this manuscript.

Disclosures. The authors declare no conflict of interest.

Data availability. Data underlying the results presented in this paper are not publicly available at this time but may be obtained from the corresponding author upon reasonable request.

References

1. R. Rampat and D. Gatinel, "Multifocal and Extended Depth-of-Focus Intraocular Lenses in 2020," Ophthalmology **128**(11), e164–e185 (2021).
2. K. M. Rocha, "Extended Depth of Focus IOLs: The Next Chapter in Refractive Technology?" J. Refract. Surg. **33**(3), 146–149 (2017).
3. D. Montagud-Martínez, V. Ferrando, A. Martínez-Espert, S. Garcia-Delpech, J. A. Monsoriu, and W. D. Furlan, "In Vitro Chromatic Performance of Three Presbyopia-Correcting Intraocular Lenses with Different Optical Designs," J. Clin. Med. **11**(5), 1212 (2022).
4. A. F. Borkenstein, E. M. Borkenstein, H. Luedtke, and R. Schmid, "Optical Bench Analysis of 2 Depth of Focus Intraocular Lenses," Biomed. Hub **6**(3), 77–85 (2021).
5. G. S. Sachdev and M. Sachdev, "Optimizing outcomes with multifocal intraocular lenses," Indian J. Ophthalmol. **65**(12), 1294–1300 (2017).

Biomedical Optics EXPRESS

6. D. Fernandez, S. Barbero, C. Dorronsoro, and S. Marcos, "Multifocal intraocular lens providing optimized through-focus performance," Opt. Lett. **38**(24), 5303–5306 (2013).
7. G.-M. Dai, "Optical surface optimization for the correction of presbyopia," Appl. Opt. **45**(17), 4184–4195 (2006).
8. J. Ares, R. Flores, S. Bará, and Z. Jaroszewicz, "Presbyopia Compensation with a Quartic Axicon," Optom. Vis. Sci. **82**(12), 1071–1078 (2005).
9. L. Romero, M. Millán, Z. Jaroszewicz, and A. Kolodziejczyk, "Double peacock eye optical element for extended focal depth imaging with ophthalmic applications," J. Biomed. Opt. **17**(4), 046013 (2012).
10. K. Petelczyc, S. Bará, A. C. Lopez, Z. Jaroszewicz, K. Kakarenko, A. Kolodziejczyk, and M. Sypek, "Imaging properties of the light sword optical element used as a contact lens in a presbyopic eye model," Opt. Express **19**(25), 25602–25616 (2011).
11. K. Petelczyc, A. Kolodziejczyk, N. Blocki, A. Byszewska, Z. Jaroszewicz, K. Kakarenko, K. Kolacz, M. Miler, A. Mira-Agudelo, W. Torres-Sepulveda, and M. Rekas, "Model of the light sword intraocular lens: in-vitro comparative studies," Biomed. Opt. Express **11**(1), 40–54 (2020).
12. P. de Gracia, C. Dorronsoro, and S. Marcos, "Multiple zone multifocal phase designs," Opt. Lett. **38**(18), 3526–3529 (2013).
13. Z. Zalevsky, A. Shemer, A. Zlotnik, E. B. Eliezer, and E. Marom, "All-optical axial super resolving imaging using a low-frequency binary-phase mask," Opt. Express **14**(7), 2631–2643 (2006).
14. H. Zhang, H. Liu, Z. Lu, and H. Zhang, "Modified phase function model for kinoform lenses," Appl. Opt. **47**(22), 4055–4060 (2008).
15. F. Castignoles, M. Flury, and T. Lepine, "Comparison of the efficiency, MTF and chromatic properties of four diffractive bifocal intraocular lens designs," Opt. Express **18**(5), 5245–5256 (2010).
16. D. Gatinel, C. Pagnoulle, Y. Houbrechts, and L. Gobin, "Design and qualification of a diffractive trifocal optical profile for intraocular lenses," J. Cataract Refractive Surg. **37**(11), 2060–2067 (2011).
17. P. Mojzis, P. Pena-Garcia, I. Liehneova, P. Ziak, and J. L. Alio, "Outcomes of a new diffractive trifocal intraocular lens," J. Cataract Refractive Surg. **40**(1), 60–69 (2014).
18. P. de Gracia, C. Dorronsoro, Á. Sánchez-González, L. Sawides, and S. Marcos, "Experimental simulation of simultaneous vision," Invest. Ophthalmol. Visual Sci. **54**(1), 415–422 (2013).
19. F. Gori, M. Santarsiero, S. Vicalvi, R. Borghi, G. Cincotti, E. D. Fabrizio, and M. Gentili, "Analytical derivation of the optimum triplicator," Opt. Commun. **157**(1-6), 13–16 (1998).
20. P. J. Valle, J. E. Oti, V. F. Canales, and M. P. Cagigal, "Visual axial PSF of diffractive trifocal lenses," Opt. Express **13**(7), 2782–2792 (2005).
21. F. Vega, M. Valentino, F. Rigato, and M. S. Millan, "Optical design and performance of a trifocal sinusoidal diffractive intraocular lens," Biomed. Opt. Express **12**(6), 3338–3351 (2021).
22. M. Sokoowski, J. Pniewski, R. Brygoa, and M. Kowalczyk-Hernández, "Hybrid heptafocal intraocular lenses," Opt. Appl. **XLV**(3), 285–298 (2015).
23. VSY Biotechnology, The Netherlands, "Acriva Trinova product brochure," https://www.vsybiotechnology.com/acriva-trinova/.
24. Hanita Lenses, Israel, "Intensity-Hanita lenses," https://www.hanitalenses.com/intraocular-implants/multifocal/intensity/.
25. A.-F. Alfredo, C.-G. Alfredo, C.-G. David, M.-S. Paula, and A. Alfredo, "Comparative study of visual results obtained with two trifocal lens models in cataract surgery," J. Clin. Res. Ophthalmol. **7**, 054–060 (2020).
26. E. Nov, A. Rubowitz, N. Dar, T. Sharon, and E. I. Assia, "Visual performance of a novel optical design of a new multifocal intraocular lens," J. Refract. Surg. **38**(3), 150–157 (2022).
27. D. Marco, M. M. Sanchez-Lopez, A. Cofre, A. Vargas, and I. Moreno, "Optimal triplicator design applied to a geometric phase vortex grating," Opt. Express **27**(10), 14472–14486 (2019).
28. H.-L. Liou and N. A. Brennan, "Anatomically accurate, finite model eye for optical modeling," J. Opt. Soc. Am. A **14**(8), 1684–1695 (1997).
29. D. A. Atchison and G. Smith, "Chromatic dispersions of the ocular media of human eyes," J. Opt. Soc. Am. A **22**(1), 29–37 (2005).
30. M.-C. Robert and P. Harasymowycz, "Intraocular Lens Position Following In-the-Bag Implantation of Single-Piece Versus Three-Piece Acrylic Intraocular Lenses," Ophthalmic Surg. Lasers Imaging **43**(6), 472–478 (2012).
31. A. Nemes-Czopf, D. Bercsenyi, and G. Erdei, "Simulation of relief-type diffractive lenses in ZEMAX using parametric modelling and scalar diffraction," Appl. Opt. **58**(32), 8931–8942 (2019).
32. C. Timar-Fulep, "Realistic modeling of relief-type diffractive intraocular lenses using User-Defined Surface DLLs," (2022) https://support.zemax.com/hc/en-us/articles/7772225130259.
33. D. A. Buralli and G. M. Morris, "Effects of diffraction efficiency on the modulation transfer function of diffractive lenses," Appl. Opt. **31**(22), 4389–4396 (1992).
34. V. Portney, "Light distribution in diffractive multifocal optics and its optimization," J. Cataract Refractive Surg. **37**(11), 2053–2059 (2011).
35. A. L. Custódio, J. F. A. Madeira, A. I. F. Vaz, and L. N. Vicente, "Direct Multisearch for Multiobjective Optimization," SIAM J. Optim. **21**(3), 1109–1140 (2011).
36. S. Ravikumar, L. N. Thibos, and A. Bradley, "Calculation of retinal image quality for polychromatic light," J. Opt. Soc. Am. A **25**(10), 2395–2407 (2008).

Biomedical Optics EXPRESS

37. "Photometry – The CIE system of physical photometry (ISO 23539:2005(E)/CIE S 010/E:2004)," (2004).
38. D. Carson, W. E. Hill, X. Hong, and M. Karakelle, "Optical bench performance of AcrySof IQ ReSTOR, AT LISA tri, and FineVision intraocular lenses," Clin Ophthalmol. **8**, 2105–2113 (2014).
39. D. Carson, Z. Xu, E. Alexander, M. Choi, Z. Zhao, and X. Hong, "Optical bench performance of 3 trifocal intraocular lenses," J. Cataract Refractive Surg. **42**(9), 1361–1367 (2016).
40. S. H. Chae, H. S. Son, R. Khoramnia, K. H. Lee, and C. Y. Choi, "Laboratory evaluation of the optical properties of two extended-depth-of-focus intraocular lenses," BMC Ophthalmol. **20**(1), 53 (2020).
41. A. F. Borkenstein, E. M. Borkenstein, and R. Schmid, "Analysis of a novel hydrophobic acrylic enhanced monofocal intraocular lens compared to its standard monofocal type on the optical bench," BMC Ophthalmol. **22**(1), 356 (2022).
42. R. Schmid, C. Fuchs, H. Luedtke, and A. F. Borkenstein, "Depth of focus of four novel extended range of vision intraocular lenses," Eur. J. Ophthalmol. **33**(1), 257–261 (2023).
43. A. Dominguez-Vicent, J. J. Esteve-Taboada, A. J. Del Aguila-Carrasco, T. Ferrer-Blasco, and R. Montes-Mico, "In vitro optical quality comparison between the Mini WELL Ready progressive multifocal and the TECNIS Symfony," Graefes Arch. Clin. Exp. Ophthalmol. **254**(7), 1387–1397 (2016).
44. M. S. Millán and F. Vega, "Extended depth of focus intraocular lens. Chromatic performance," Biomed. Opt. Express **8**(9), 4294–4309 (2017).
45. C. C. Vidal, A. A. Heredia, P. A. Piers, and H. A. Weebe, "Progressive power intraocular lens, and methods of use and manufacture," (April 2020).
46. P. Artal, S. Manzanera, P. Piers, and H. Weeber, "Visual effect of the combined correction of spherical and longitudinal chromatic aberrations," Opt. Express **18**(2), 1637–1648 (2010).
47. Y. Zhai, Y. Wang, Z. Wang, Y. Liu, L. Zhang, Y. He, and S. Chang, "Design of eye models used in quantitative analysis of interaction between chromatic and higher-order aberrations of eye," Opt. Commun. **332**, 89–95 (2014).
48. N. Suchkov, E. J. Fernández, and P. Artal, "Impact of longitudinal chromatic aberration on through-focus visual acuity," Opt. Express **27**(24), 35935–35947 (2019).
49. G.-Y. Yoon and D. R. Williams, "Visual performance after correcting the monochromatic and chromatic aberrations of the eye," J. Opt. Soc. Am. A **19**(2), 266–275 (2002).
50. L. N. Thibos, A. Bradley, and X. Zhang, "Effect of Ocular Chromatic Aberration on Monocular Visual Performance," Optom. Vis. Sci. **68**(8), 599–607 (1991).
51. G. Labuz, N. J. Reus, and T. J. T. P. van den Berg, "Comparison of ocular straylight after implantation of multifocal intraocular lenses," J. Cataract Refract Surg. **42**(4), 618–625 (2016).
52. V. Osipov, L. L. Doskolovich, E. A. Bezus, W. Cheng, A. Gaidukeviciute, and B. Chichkov, "Fabrication of three-focal diffractive lenses by two-photon polymerization technique," Appl. Phys. A **107**(3), 525–529 (2012).
53. V. P. Osipov, L. L. Doskolovich, E. A. Bezus, T. E. Drew, K. Zhou, K. Sawalha, G. Swadener, and J. S. W. Wolffsohn, "Application of nanoimprinting technique for fabrication of trifocal diffractive lens with sine-like radial profile," J. Biomed. Opt. **20**(2), 025008 (2015).
54. J. Xie, *Design, Fabrication and Testing of Diffractive Multifocal Intraocular Lens (MIOL)* (The University of Arizona, 2018).
55. J. Fernandez, J. Garcia-Montesinos, J. Martinez, D. P. Pinero, and M. Rodriguez-Vallejo, "Posterior capsular opacification evaluation through contrast sensitivity defocus curves with two multifocal intraocular lenses of similar material," Graefe's Arch. Clin. Exp. Ophthalmol. **259**(10), 2995–3002 (2021).
56. R. Mukherjee, K. Chaudhury, S. Das, S. Sengupta, and P. Biswas, "Posterior capsular opacification and intraocular lens surface micro-roughness characteristics: an atomic force microscopy study," Micron **43**(9), 937–947 (2012).
57. "Ophthalmic implants - Intraocular lenses - Part 2: Optical properties and test methods (ISO 11979-2:2014)," (2015).
58. J. B. Ale, "Intraocular lens tilt and decentration: a concern for contemporary IOL designs," Nepal. J. Ophthalmol. **3**(1), 68–77 (1970).